A New Prediction Model for Tropical Storm Frequency over the Western North Pacific Using Observed Winter-Spring Precipitation and Geopotential Height at 500 hPa*

WANG Huijun† (王会军)

Institute of Atmospheric Physics, Chinese Academy of Sciences, Beijing 100029

(Received March 19, 2010; in final form March 22, 2011)

ABSTRACT

A new seasonal prediction model for annual tropical storm numbers (ATSNs) over the western North Pacific was developed using the preceding January-February (JF) and April-May (AM) grid-point data at a resolution of $2.5° \times 2.5°$. The JF and AM mean precipitation and the AM mean 500-hPa geopotential height in the Northern Hemisphere, together with the JF mean 500-hPa geopotential height in the Southern Hemisphere, were employed to compose the ATSN forecast model via the stepwise multiple linear regression technique. All JF and AM mean data were confined to the Eastern Hemisphere. We established two empirical prediction models for ATSN using the ERA40 reanalysis and NCEP reanalysis datasets, respectively, together with the observed precipitation. The performance of the models was verified by cross-validation. Anomaly correlation coefficients (ACC) at 0.78 and 0.74 were obtained via comparison of the retrospective predictions of the two models and the observed ATSNs from 1979 to 2002. The multi-year mean absolute prediction errors were 3.0 and 3.2 for the two models respectively, or roughly 10% of the average ATSN. In practice, the final prediction was made by averaging the ATSN predictions of the two models. This resulted in a higher score, with ACC being further increased to 0.88, and the mean absolute error reduced to 1.92, or 6.13% of the average ATSN.

Key words: tropical storm, frequency, western North Pacific, seasonal prediction

Citation: Wang Huijun, 2011: A new prediction model for tropical storm frequency over the western North Pacific using observed winter-spring precipitation and geopotential height at 500 hPa. *Acta Meteor. Sinica*, **25**(3), 262–271, doi: 10.1007/s13351-011-0302-6.

1. Introduction

The tropical cyclone (TC) activity has strong interannual variability (e.g., Landsea et al., 1999), making its seasonal prediction very challenging. Naturally, such predictions must rely on an understanding of the physical processes associated with the variability in the TC activity. Many results have been reported with respect to the roles of El Niño–Southern Oscillation (ENSO) (Chan, 1985, 2000; Dong, 1988; Wu and Lau, 1992; Lander, 1993, 1994; Wang and Chan, 2002; Camargo and Sobel, 2004) and the quasi-biennial oscillation in the stratosphere (Chan, 1995). Other studies have revealed the link between the TC activity and large-scale atmospheric variability (Ding, 1983; Briegel and Frank, 1997; Ritchie and Holland, 1998; Vimont and Kossin, 2007) such as the North Atlantic Oscillation (Elsner and Kocher, 2000), North Pacific Oscillation and sea ice coverage (Wang et al., 2007; Fan, 2007), Antarctic Oscillation (Wang and Fan, 2007), Hadley circulation (Zhou et al., 2008a), and land-sea thermal contrast (Zhou et al., 2008b; Zou and Zhao, 2009).

Prediction studies of the TC activity have been performed for both the Atlantic (e.g., Gray et al., 1992; Elsner and Schmertmann, 1993; Thorncroft and Pytharoulis, 2001; Wang and Qian, 2010; Fan and Wang, 2010) and the western North Pacific (WNP) (e.g., Chan et al., 1998, 2001; Fan and Wang, 2009). The models set up by Chan et al. (1998, 2001) and

*Supported by the National Basic Research Program of China (2009CB421406) and National Natural Science Foundation of China (40875048 and 40775049).

†Corresponding author: wanghj@mail.iap.ac.cn.

(Chinese version to be published)

©The Chinese Meteorological Society and Springer-Verlag Berlin Heidelberg 2011

Fan and Wang (2009) for the WNP TC frequency are based on the selected indices representing the ENSO phase, quasi-biennial oscillation, and the large-scale atmospheric circulation. These models have all been demonstrated to have reasonable forecasting skills.

However, the physical processes involved in the TC activity are complex, and the climate regimes may change due to long-term variability. As a result, the dominating factors may not be stable from time to time. Thus, we need to develop new models, which differ from most of the previous models in that they do not adopt fixed predictor sets. In this paper, we intend to establish a new forecast model for annual tropical storm numbers (ATSNs) in the WNP by using the global grid-point data of precipitation and 500-hPa geopotential height.

The main criterion for defining a tropical storm is that it must have the maximum wind speed exceeding 17 m s^{-1}. The observation data for ATSNs were obtained from the Joint Typhoon Warning Center (JTWC). The region of the WNP was confined to the area of 5°–45°N, 105°–180°E, including the South China Sea. The US Climate Prediction Center (CPC) Merged Analysis of Precipitation (CMAP) data (Xie and Arkin, 1997) and the 500-hPa geopotential height (GH5) in the ERA40 and NCEP/NCAR reanalysis were employed in this study. Reliable global precipitation data are available only after 1979 and the ERA40 dataset stops in 2002. Thus, the present study utilized GH5 and precipitation data from 1979–2002. Anomaly correlation coefficient (ACC) between the prediction and observation, mean absolute error (MAE), and root mean square error (RMSE) were used to evaluate the prediction skill. We also used the data of outgoing long-wave radiation (OLR) at the top of the atmosphere from NOAA. In this paper, all anomaly fields refer to the deviations relative to the 1979–2002 average.

The Antarctic Oscillation (AAO) is defined as the leading principal component of 850-hPa geopotential height anomalies south of 20°S (Thompson and Wallace, 2000; data source: http://jisao.washington.edu/data/aao/♯data). The monthly Arctic Oscillation (AO) index was constructed by projecting the daily 1000-hPa height anomalies poleward of 20°N onto the AO loading pattern (Higgins et al., 2002; data source: http://www.cpc.ncep.noaa.gov/products/precip/CW link/daily_ao_index/ao.shtml).

2. Predictors

The January-February (JF) and April-May (AM) precipitation and 500-hPa geopotential height can be used to compose the forecast model of ATSN. This arises from their relationship to ATSN via changes in the convective activity and atmospheric circulation over the WNP. First, the correlation coefficient (CC) between JF and AM precipitation versus ATSN was computed and plotted (Fig. 1). The ATSN was significantly associated with JF and AM precipitation over the WNP. JF precipitation in central eastern China was also linked to the ATSN. In addition, AM precipitation in North Africa was associated with the ATSN. In this paper, we provide an explanation for this precipitation-ATSN relationship based on OLR analysis, as shown in Figs. 3–7.

JF mean GH5 over the large area of the Southern Hemisphere was connected with the ATSN (Fig. 2a). The geographical pattern highly resembles the AAO (or Southern Annular Mode). Wang and Fan (2007) have documented the relationship between the annual WNP typhoon frequency and the AAO during the boreal summer. They found that variations in AAO are associated with atmospheric circulation changes in the tropical Pacific. Fan (2009) further indicated a similar relationship between the Western Hemisphere portion of AAO and the annual hurricane frequency in the tropical Atlantic. Therefore, the AAO, as a major mode in the Southern Hemisphere, is quite influential on TC activities. In fact, the JF AAO and ATSN were significantly correlated with CC = 0.39 between 1979 and 2002 (CC = 0.30 between 1950 and 2002). The AM AAO was also correlated with ATSN, but with a smaller CC value (0.29 and 0.30, respectively, for the periods of 1979–2002 and 1950–2002). The coherence of JF AAO and ATSN can be seen clearly in Fig. 3.

Figure 2b relates the preceding AM GH5 signals

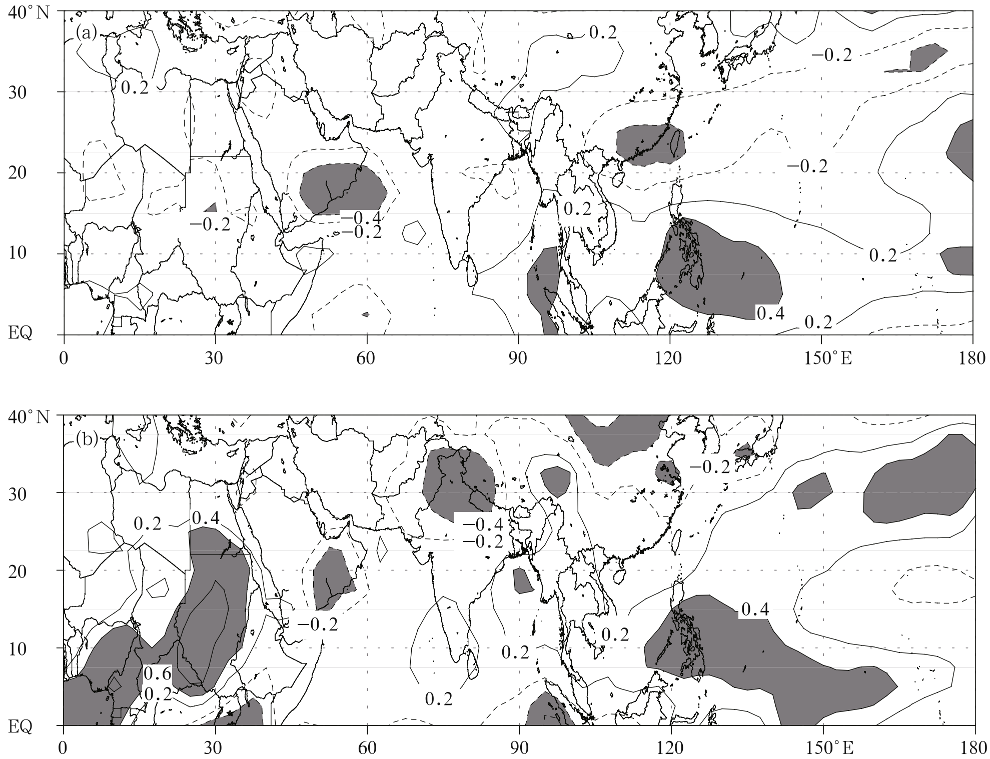

Fig. 1. Spatial distributions of the CC between the ATSN and JF precipitation (a) and AM precipitation (b). Areas with CC larger than 0.4 at the significance level over 95% are shaded.

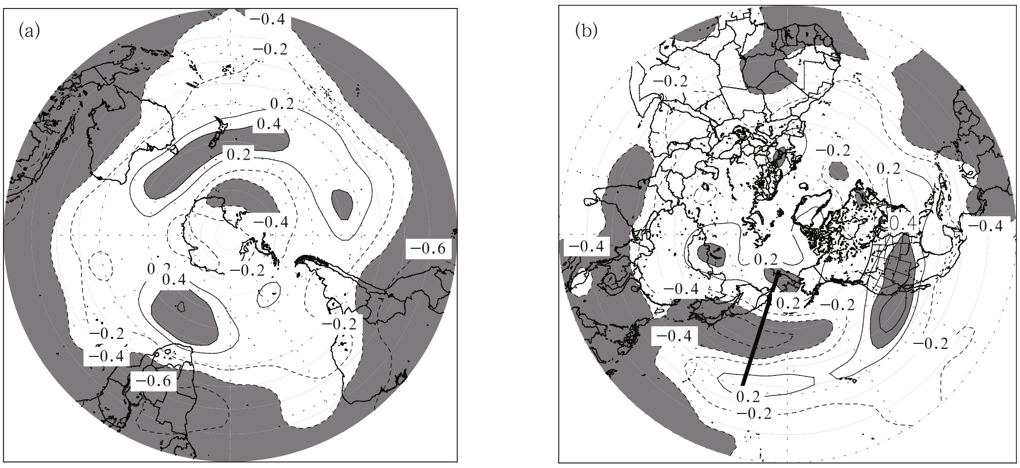

Fig. 2. Spatial distributions of the CC between the ATSN and JF GH5 in the Southern Hemisphere (a) and AM GH5 in the Northern Hemisphere (b). GH5 is from ERA40. Areas with CC larger than 0.4 at the significance level over 95% are shaded.

over the Northern Hemisphere with pronounced information of ATSN at low latitudes and in the central North Pacific. The spatial pattern over the central North Pacific was characterized by a north-south distribution, as indicated by a thick beeline, shaping the North Pacific Oscillation (NPO) pattern. As revealed by Wang et al. (2007), the NPO during the boreal summer is positively correlated with the WNP

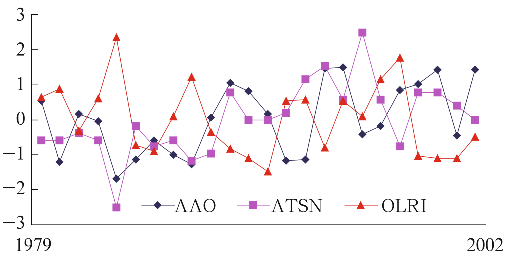

Fig. 3. Normalized time series of JF AAO, ATSN, and OLRI for 1979–2002. The OLRI is defined as the mean June-October OLR averaged over the region of 10°–22.5°N, 130°–160°E.

typhoon frequency. This occurs because of the zonal wind variability and the change in the magnitude of vertical zonal wind shear between high and low levels in the troposphere. Our discussion here, based on Fig. 2b, is consistent with their finding. Furthermore, the computed CC between the AM NPO index, as defined by the normalized sea level pressure (data from the Hadley Center) difference between (65°N, 170°E) and (25°N, 165°E) (Wallace and Gutzler, 1981), and the ATSN was also significant (0.31) for the period 1945–1998. This period was selected for CC computation here because of the temporal coverage of the Hadley Center sea level pressure data. The CC between the AM NPO and the WNP tropical storm number from June to October (JJASO) was 0.36. This further demonstrates the AM NPO signal in influencing the WNP tropical storm activity on the interannual scale.

The aforementioned relationships can now be discussed in the context of convective activity that is closely associated with tropical storm formations. Positive ATSN anomalies are definitely associated with stronger than normal convective activities in the WNP, and vice versa. Thus, we obtained negative CCs between the ATSN and OLR averaged for JJASO in the major tropical storm genesis region of the WNP (Fig. 4). An index was defined as the averaged OLR over the region of 10°–22.5°N, 130°–160°E, hereafter referred to as OLRI, which also adequately represented convective activities and the ATSN over the WNP (see Figs. 4 and 5). The ATSN and annual mean OLRI were correlated with CC = –0.58 in the period 1979–2002. The JJASO mean OLRI was correlated with ATSN at CC = –0.44. The ATSN and JJASO OLRI series (see Table 1) demonstrate their coherence, particularly for years with large anomalies.

Subsequently, we analyzed the preceding JF and AM precipitation signals in JJASO OLRI. We found that strong signals of precipitation in JF and AM were located in large areas of the western Pacific (Fig. 6). Signals in the tropical western Pacific were even stronger (with larger CCs, as shown in Fig. 6) in AM than in JF. Therefore, the signals appeared in JF, developed in AM, and persisted until the JJASO season. This is the physical background for the relationship between the preceding precipitation and ATSN.

The preceding signals for the OLRI of JJASO existed in the GH5 as well. Figure 7a nicely illustrates this consequence. The spatial pattern for the JF case resembles that of the AAO in the middle and high latitudes of the Southern Hemisphere. The association between the AAO and OLR over the tropical western Pacific has been addressed in our recent paper (Sun et al., 2009). In this context, the convective activity over the Maritime Continent serves as a bridge to link the variability of mid and high latitude circulations in the Southern Hemisphere and the convective activity over

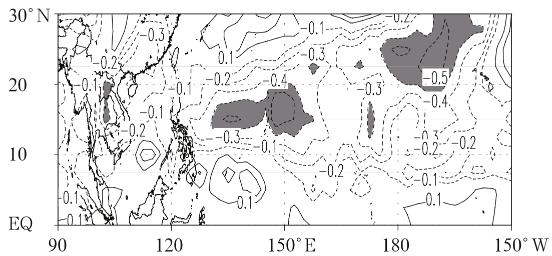

Fig. 4. Spatial distribution of the CC between the ATSN and the JJASO mean OLR. Areas with CC larger than 0.4 at the significance level over 95% are shaded.

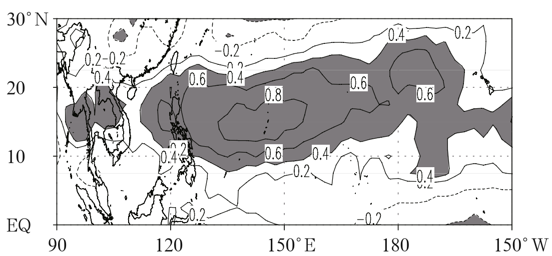

Fig. 5. As in Fig. 4, but for the CC between the OLRI and the JJASO mean OLR.

Table 1. The observed and predicted ATSN anomalies with PRD1 (obsa and prda, respectively), their differences (obs–prd), relative errors, OLR index, and number of predictors for the years of 1979–2002. All values for the prediction were obtained from the model established for every year using data from the remaining 23 years

Year	prda	obsa	obs–prd	Relative error	OLR index	Number of predictors
1979	–8.14	–3.04	4.72	20.29%	0.62	16
1980	–1.06	–3.04	–2.36	–7.78%	0.86	17
1981	–0.23	–2.04	–2.19	–7.03%	–0.32	16
1982	–2.50	–3.04	–0.92	–3.19%	0.60	16
1983	–13.52	–13.04	0.10	0.53%	2.35	17
1984	1.88	–1.04	–3.31	–9.92%	–0.74	16
1985	–5.67	–4.04	1.25	4.85%	–0.90	17
1986	–13.52	–13.04	0.10	0.53%	2.35	17
1984	2.84	–3.04	–6.27	–18.28%	0.07	17
1987	–1.65	–6.04	–4.77	–16.03%	1.20	18
1988	–10.30	–5.04	4.88	23.11%	–0.35	17
1989	10.28	3.96	–6.70	–16.06%	–0.83	16
1990	0.83	–0.04	–1.25	–3.86%	–1.13	18
1991	0.73	–0.04	–1.15	–3.59%	–1.48	17
1992	–0.18	0.96	0.76	2.43%	0.52	16
1993	7.39	5.96	–1.81	–4.65%	0.56	16
1994	2.08	7.96	5.50	16.41%	–0.80	17
1995	–1.99	2.96	4.57	15.51%	0.53	18
1996	10.53	12.96	2.05	4.88%	0.10	17
1997	4.37	2.96	–1.79	–5.01%	1.16	16
1998	1.79	–4.04	–6.21	–18.70%	1.76	16
1999	3.50	3.96	0.08	0.23%	–1.03	16
2000	6.06	3.96	–2.48	–6.62%	–1.12	17
2001	–2.84	1.96	4.42	15.48%	–1.12	17
2002	–4.22	–0.04	3.80	13.98%	–0.51	16
Average			MAE = 3.06	MAE in percentage = 9.74%		

the WNP. Such a linkage is valid in both the lower and higher troposphere. Therefore, the GH5 in the Southern Hemisphere can be adopted as a predictor for the tropical storm activity over the WNP.

As shown in Fig. 7b, the early signal in AM exists primarily over the low latitudes and North Pacific sector. Therefore, we also used AM GH5 in the Northern Hemisphere as a type of predictor for ATSN. Again, the thick beeline in the figure indicates the meridional pattern, similar to that shown in Fig. 2b. Thus, there are early signals in AM GH5, particularly the meridional pattern over the western Pacific in the OLRI variability for JJASO.

3. Prediction and cross-validation procedures

Grid-point data for the JF and AM mean precipitation, the AM GH5 in the region 10°S–80°N, 0°–180°E, and the JF GH5 in the region 10°N–80°S, 0°–180°E, were employed to establish the forecast model for the ATSN in the WNP via the stepwise multiple regression technique. The forecast model for ATSN was set up for every year using data from the remaining 23 years. Thus, we were able to carry out the cross-validation to assess the model performance. For each individual year, 16–18 independent predictors were finally selected to compose the prediction model after the stepwise regression. On average, there were four or five predictors from each of the four fields, namely, JF precipitation, AM precipitation, and their corresponding GH5.

Therefore, we developed two models (PRD1 and PRD2) for the prediction of ATSN using the ERA40 and NCEP reanalysis, respectively, together with the CMAP precipitation data. First, we will discuss verification of the prediction by PRD1 (established using the ERA40 GH5). The ACC between the prediction and observation was 0.78. The detailed results of the

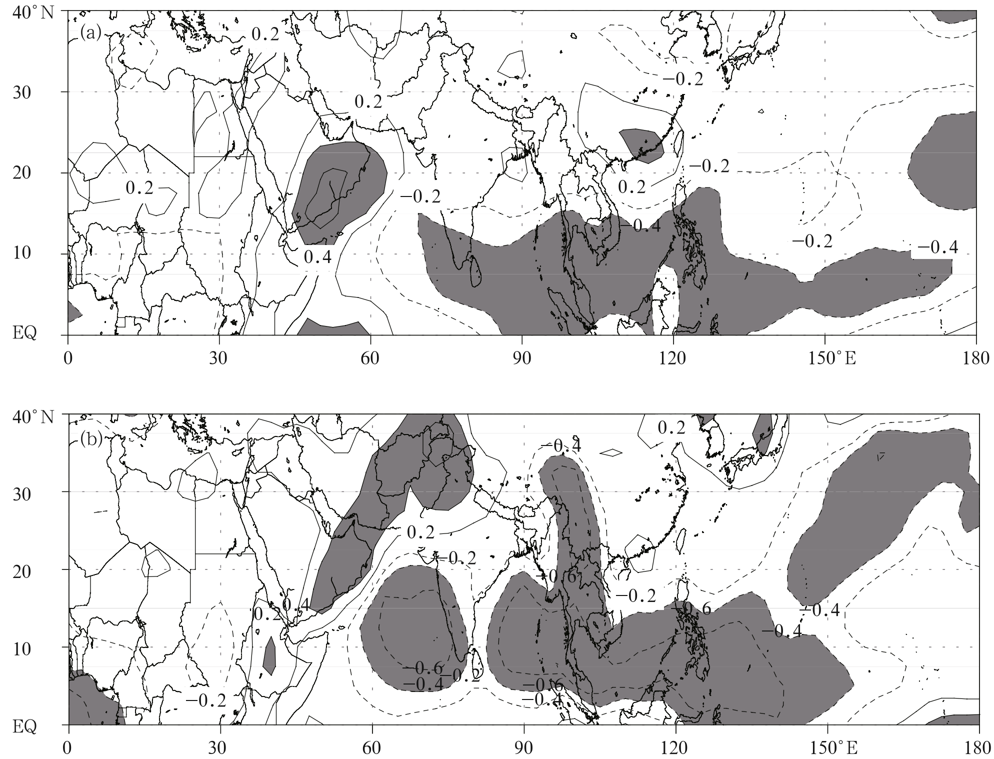

Fig. 6. As in Fig. 1, but with ATSN replaced by OLRI.

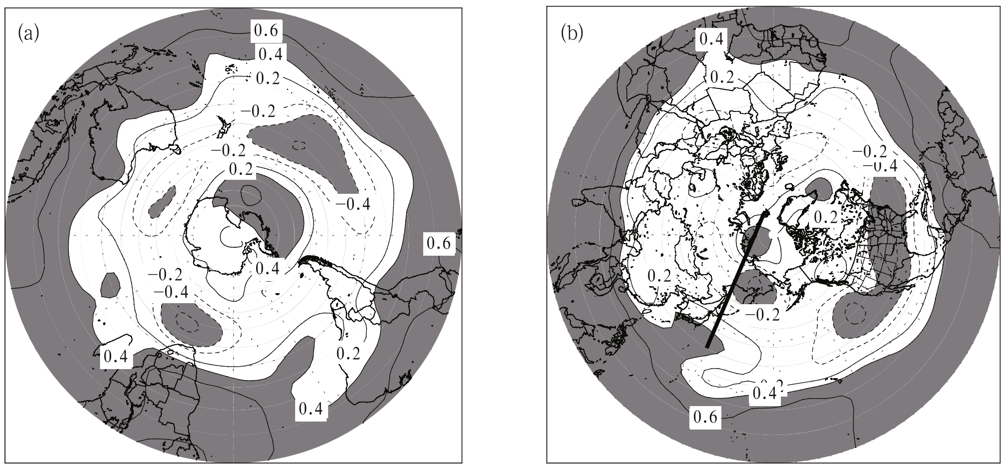

Fig. 7. As in Fig. 2, but with ATSN replaced by OLRI.

cross-validation are listed in Table 1. The multi-year predicted average ATSN was 31.04, which is almost the same as the observation (31.42). The 24-yr MAE was 3.06, or 9.7% of the observed average ATSN (31.42). The RMSE of the predictions was 3.62, or 11.55% of the mean observed ATSN. Predictions were particularly good for the years 1982, 1983, 1985, 1990–1993, 1997, and 1999, with absolute errors less than 2.0. The signs for all the years with large anomalies (1983, 1987, 1988, 1993, 1994, and 1996) were correctly predicted, which is particularly important for operational applications.

It is also worth noting that the observed ATSN experienced a notable interdecadal variation at the end of the 1980s. The ATSN was less than or equal to 30 between 1979 and 1988. However, it was larger than 30 in the following years, with 1991 an exception with a much lower ATSN. Thus, the ATSN was significantly larger in the later period compared with the former one. The model can reasonably capture this interdecadal variation, as shown in Fig. 8 and Table 1, despite some quantitative discrepancies.

Figure 9 shows a plot of all grid points where the precipitation and ERA40 GH5 data were finally selected as predictors from 1979 to 2002. The four panels indicate the JF precipitation, AM precipitation, and GH5 for each period, respectively. As discussed above, only 4–6 grid points from one panel were finally selected as the predictors for every year in the stepwise multiple regression process. Each panel of Fig. 9 includes the predictors of all 24 years. The distribution of the predictors was spatially diverse from year to year. Therefore, we conclude that the predictor suite from any field (GH5 in JF or AM, or precipitation in JF or AM) is quite different from year to year. This reflects the physical complexity of the climate variability and predictability. As a result, the dominating factors for the ATSN change from time to time. Therefore, it is advantageous of our current approach to employ the stepwise multiple regression technique based on all the grid points, GH5, and precipitation data.

Besides the tropical predictors, our approach also considers the high-latitude predictors, as represented by those in the GH5. High-latitude predictors may well reflect the co-variability of the climate over high latitudes and the WNP region, e.g., the association between the AAO and ATSN activity, as indicated by Wang and Fan (2007).

4. Approach to obtain an even higher predictive skill

The established model, as described in the previous section, employs the JF and AM observed precipitation and the ERA40 GH5. Here, we also established another ATSN prediction model (PRD2) in the same way, but using NCEP reanalysis GH5 data. A cross-validation of the models was carried out. The ACC between the new model predicted ATSN and the observed ATSN was 0.74, which is a little lower than the previous model (PRD1). The MAE and the RMSE were 3.16 and 3.84 (i.e., 10.08% and 12.25% of the average ATSN), respectively. Thus, the skill was a little lower and the errors were a little larger, as compared to the results of PRD1.

An interesting question arises because of this. Namely, can we further improve the ATSN prediction by averaging the results of the two models? The answer is " yes". The ACC between the averaged prediction and the observation was 0.88, which is an exciting score. The MAE and RMSE were 1.92 and 2.51 (i.e., 6.13% and 8.01% of the average ATSN), respectively. The detailed results of the PRD1 and PRD2 models for the years 1979–2002 are depicted in Fig. 8.

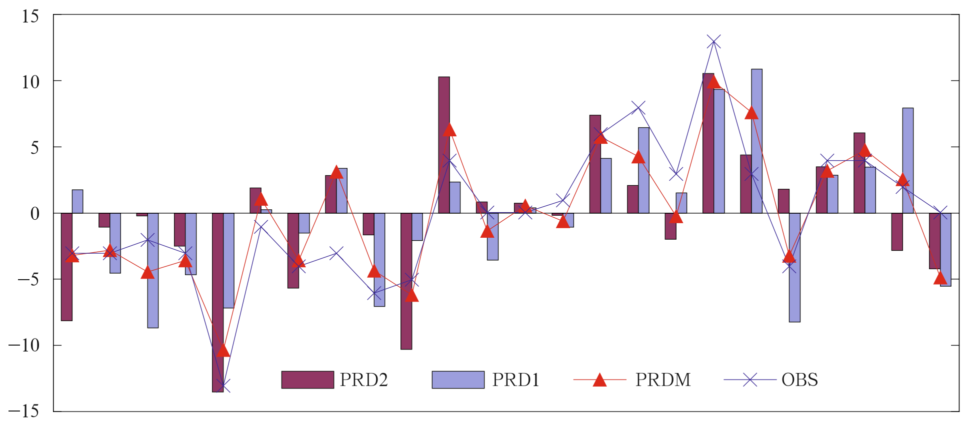

Fig. 8. Time series of observed (OBS) and model predicted ATSN, in which PRD1 stands for the model established using the JF and AM precipitation and EAR40 GH5. PRD2 stands for the model established using the JF and AM precipitation and NCEP reanalysis GH5. PRDM denotes the mean of PRD1 and PRD2. The model predicted ATSN was obtained retrospectively in the cross-validation of the model established for every year using data from the remaining 23 years.

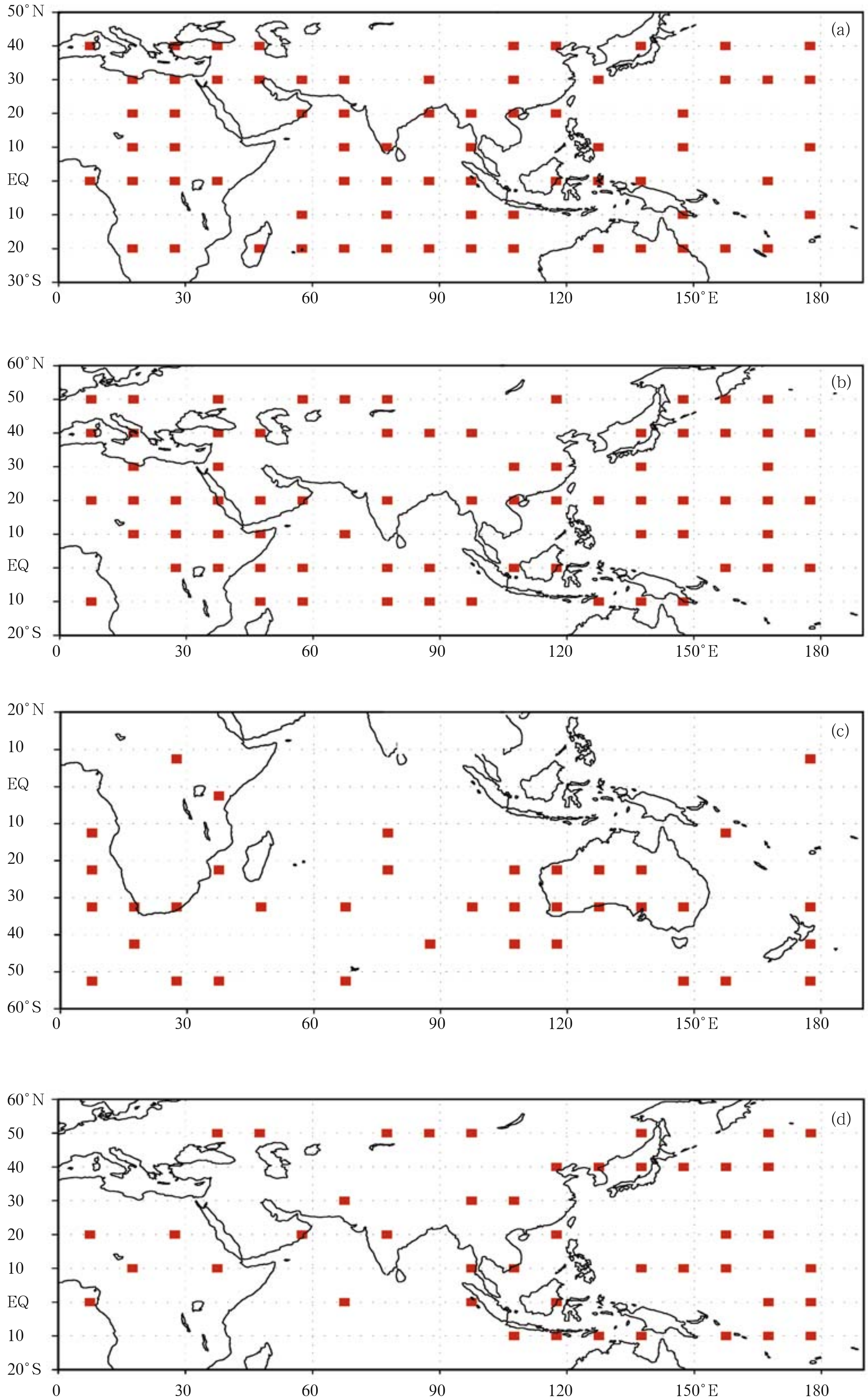

Fig. 9. Spatial locations of the ultimately selected predictors of ATSN for the years 1979–2002: (a) JF mean precipitation, (b) AM mean precipitation, (c) JF mean ERA40 GH5, and (d) AM mean ERA40 GH5. These were taken via the stepwise multiple regression performed every year using data from the remaining 23 years.

Therefore, our ensemble approach (each model was established using the preceding CMAP precipitation together with reanalyzed GH5 data from ERA40 and NCEP) is quite effective in the prediction of WNP ATSN. It should be interesting to verify the effectiveness of this new approach toward climate predictions for other quantities, such as TC numbers in other oceanic sectors and the precipitation in monsoon regions.

5. Conclusions

In this study, we proposed a new forecasting approach for the annual tropical storm number in the western North Pacific. This was carried out using the preceding January-February and April-May mean precipitation in the Northern Hemisphere and the 500-hPa geopotential height for the JF mean in the Southern Hemisphere and AM mean in the Northern Hemisphere. All grid-point data of precipitation and GH5 were from the eastern portion of the globe. The stepwise multiple linear regression technique was used. Finally, 16–18 predictors were selected to compose the ATSN forecast model for every year during the cross-validation period from 1979 to 2002. Two parallel models (PRD1 and PRD2) were constructed by adopting the ERA40 and NCEP reanalysis data, respectively. The anomaly correlation coefficient between the observed and retrospectively predicted ATSN by PRD1 was 0.78, with a multi-year MAE of 3.06. Similar skill was obtained when the PRD2 was applied. The prediction skill scores presented here are acceptable.

The most important finding of this research, from the perspective of operational prediction of ATSN, is that we have found a new approach with a high predictive skill. When adopting the average prediction of the two models established in this investigation, the prediction is quite consistent with the observation, with the ACC at 0.88 and the MAE at 1.92 (i.e., 6.13%). In addition to the high accuracy of the predictions, the procedure of this approach is simple and easy for operational implementation.

In this paper, we also briefly described and justified the usage of the preceding precipitation and GH5. Associated principle processes include the preceding signals from high latitudes of the Northern and Southern Hemisphere, particularly the Antarctic Oscillation and North Pacific Oscillation, via changes in the tropical western Pacific (OLR in particular). The associated correlations have been partly addressed by some previous work (e.g., Sun et al., 2009). In addition, the relationship between the boreal winter and spring high-latitude climate variability and WNP tropical storm activities was demonstrated in this paper.

REFERENCES

Briegel, L. M., and W. M. Frank, 1997: Large-scale influences on tropical cyclone-genesis in the western North Pacific. *Mon. Wea. Rev.*, **125**, 1397–1413.

Camargo, S. L., and A. H. Sobel, 2004: Western North Pacific tropical cyclone intensity and ENSO. *J. Climate*, **18**, 2996–3006.

Chan, J. C. L., 1985: Tropical cyclone activity in the Northwest Pacific in relation to the El Niño/Southern Oscillation phenomenon. *Mon. Wea. Rev.*, **113**, 599–606.

——, 1995: Tropical cyclone activity in the western North Pacific in relation to El Niño and La Niña phenomenon. *Mon. Wea. Rev.*, **123**, 2567–2571.

——, 2000: Tropical cyclone activity over the western North Pacific associated with El Niño and La Niña events. *J. Climate*, **13**, 2960–2927.

——, J. N. Shi, and C. M. Lam, 1998: Seasonal forecasting of tropical cyclone activity over the western North Pacific and the South China Sea. *Wea. Forecasting*, **13**, 997–1004.

——, J. N. Shi, and K. S. Liu, 2001: Improvements in the seasonal forecasting of tropical cyclone activity over the western North Pacific. *Wea. Forecasting*, **16**, 491–498.

Ding, Y. H., 1983: The large-scale circulation conditions for the western North Pacific typhoon formation. *Acta Oceanogr. Sinica*, **5**, 561–574. (in Chinese)

Dong, K. Q., 1988: El Niño and tropical cyclone frequency in the Australian region and the Northwest Pacific. *Aust. Meteor. Mag.*, **28**, 219–225.

Elsner, J. B., and B. Kocher, 2000: Global tropical cyclone activity: A link to the North Atlantic Oscillation. *Geophys. Res. Lett.*, **27**, 128–132.

——, and C. P. Schmertmann, 1993: Improving extended-range seasonal predictions of intense Atlantic hurricane activity. *Wea. Forecasting*, **8**, 345–351.

Fan, K., 2007: North Pacific sea ice cover, a predictor for the western North Pacific typhoon frequency? *Sci. China (Ser. D)*, **50** 1251–1257.

——, 2009: Linkage between the Atlantic tropical hurricane frequency and the Antarctic oscillation in the Western Hemisphere. *Atmos. Ocean. Sci. Lett.*, **2**, 159–164.

——, and H. J. Wang, 2009: A new approach to forecasting typhoon frequency over the western North Pacific. *Wea. Forecasting*, **24**, 974–978, doi: 10.1175/2009WAF2222194.1.

——, and ——, 2010: A prediction model for the Atlantic basin tropical storm frequency using a year-to-year increment approach. *Wea. Forecasting*, **25**, doi: 10.1175/2009WAF2222406.

Gray, W. M., C. W. Landsea, P. W. Mielke, and K. J. Berry, 1992: Predicting Atlantic seasonal hurricane activity 6–11 months in advance. *Wea. Forecasting*, **7**, 440–455.

Higgins, R. W., A. Leetmaa, and V. E. Kousky, 2002: Relationships between climate variability and winter temperature extremes in the United States. *J. Climate*, **15**, 1555–1572.

Landsea, C. W., R. A. Pielke Jr., A. M. Mestas-Nuñez, and J. A. Knaff, 1999: Atlantic basin hurricanes: Indices of climatic changes. *Climatic Change*, **42**, 89–129.

Lander, M. A., 1993: Comments on "A GCM simulation of the relationship between tropical storm formation and ENSO." *Mon. Wea. Rev.*, **121**, 2137–2143.

——, 1994: An exploratory analysis of the relationship between tropical storm formation in the western North Pacific and ENSO. *Mon. Wea. Rev.*, **122**, 636–651.

Ritchie, E. A., and G. J. Holland, 1998: Large-scale patterns associated with tropical cyclogenesis in western Pacific. *Mon. Wea. Rev.*, **127**, 2027–2043.

Sun, J. Q., H. J. Wang, and W. Yuan, 2009: A possible mechanism for the co-variability of the boreal spring Antarctic Oscillation and the Yangtze River valley summer rainfall. *Int. J. Climatol.*, **29**, 1276–1284.

Thompson, D. W. J., and J. M. Wallace, 2000: Annular modes in the extratropical circulation. Part I: Month-to-month variability. *J. Climate*, **13**, 1000–1016.

Thorncroft, C., and I. Pytharoulis, 2001: A dynamical approach to seasonal prediction of Atlantic tropical cyclone activity. *Wea. Forecasting*, **16**, 725–734.

Vimont, D. J., and J. P. Kossin, 2007: The Atlantic meridional mode and hurricane activity. *Geophys. Res. Lett.*, **34**, L07709, doi:10.1029/2006GL029683.

Wallace, J. M., and D. S. Gutzler, 1981: Teleconnections in the geopotential height field during the Northern Hemisphere winter. *Mon. Wea. Rev.*, **109**, 784–812.

Wang, B., and J. C. L. Chan, 2002: How does ENSO regulate tropical storm activity over the western North Pacific. *J. Climate*, **15**, 1643–1658.

Wang, H. J., and K. Fan, 2007: Relationship between the Antarctic oscillation and the western North Pacific typhoon frequency. *Chinese Science Bulletin*, **52**, 561–565.

——, J. Q. Sun, and K. Fan, 2007: Relationships between the North Pacific Oscillation and typhoon and hurricane frequencies. *Sci. China (Ser. D)*, **50**, 1409–1416.

——, and Z. L. Qian, 2010: A potential high-score scheme for the prediction of Atlantic storm activity. *Atmos. Ocean. Sci. Lett.*, **3**(2), 116–119.

Wu, G. X., and N. C. Lau, 1992: A GCM simulation of the relationship between tropical storm formation and ENSO. *Mon. Wea. Rev.*, **120**, 958–977.

Xie, P., and P. A. Arkin, 1997: Global precipitation: A 17-year monthly analysis based on gauge observations, satellite estimates, and numerical model outputs. *Bull. Amer. Meteor. Soc.*, **78**, 2539–2558.

Zhou, B. T., X. Cui, and P. Zhao, 2008a: Relationship between the Asian-Pacific oscillation and the tropical cyclone frequency in the western North Pacific. *Sci. China (Ser. D)*, **38**, 118–123.

——, ——, and ——, 2008b: Hadley circulation signal in the tropical cyclone frequency over the western North Pacific. *J. Geophys. Res.*, **113**, D16107, doi:10.1029/2007JD009156.

Zou, Y., and P. Zhao, 2009: Relation of summer Asian Pacific oscillation to tropical cyclone activities over the coastal waters of China. *Acta Meteor. Sinica*, **67**(5), 708–715. (in Chinese)